7541

N91-22329

CONTROL EFFORT ASSOCIATED WITH MODEL REFERENCE ADAPTIVE CONTROL FOR VIBRATION DAMPING

Richard Scott Messer and Raphael T. Haftka
Department Of Aerospace and Ocean Engineering
Virginia Polytechnic Institute and State University
Blacksburg, Virginia 24060

SUMMARY

The performance of Model Reference Adaptive Control (MRAC) is studied in numerical simulations with the objective of understanding the effects of differences between the plant and the reference model. MRAC is applied to two structural systems with adjustable error between the reference model and the actual plant. Performance indices relating to control effort and response characteristics are monitored in order to determine what effects small errors have on the control effort and performance of the two systems. It is shown that reasonable amounts of error in the reference model can cause dramatic increases in both the control effort and response magnitude (as measured by energy integrals) of the plant

INTRODUCTION

During the past decade, researchers have shown much interest in control and identification of large flexible structures, with emphasis on Large Space Structure (LSS). Furthermore, our inability to model these large structural systems accurately has generated extensive research into adaptive controllers capable of maintaining stability in the face of large structural uncertainties as well as changing structural characteristics. However, most of this research has been strictly theoretical in nature (e.g., refs. 1-10) and experimental verification (e.g., refs. 11,12) of the proposed theories is lagging far behind. In addition, the focus of most theoretical research has been on designing stable adaptive controllers with little or no concern for the issue of control effort.

While it is possible to design an adaptive controller that will stabilize a structure even if we have a very poor model, the control effort may be very high. The objective of the present paper is to study the correlation between the control effort and the fidelity of the structural model. Specifically, the first step is to demonstrate that the effort associated with an adaptive control system is sensitive to knowledge of the structure. For this purpose the popular Model Reference Adaptive Control (MRAC) method was selected and two examples were studied in detail. In this paper, we monitor four performance indices: Maximum Control Force, Quadratic Control Effort, Kinetic Energy, and Potential Energy. These performance indices allow us to evaluate the effects of errors in the theoretical model. Numerical simulations were used to see how each performance index changed when errors were introduced into the system. Section II summarizes the MRAC algorithm, section III shows how a simply supported beam can be sensitive to the choice of Reference Models, section IV presents the sensitivity of a more complicated structure and section V provides concluding remarks.

MODEL REFERENCE ADAPTIVE CONTROL

Adaptive controllers generally fall into two classifications, direct and indirect. The basic difference between the two classifications is system identification. Indirect adaptive methods (e.g., refs. 9-10, 13-14) require system identification before the adaptive gains in the controller can be updated, whereas direct methods (refs. 1-8, 11-12) do not use system identification. MRAC is one of the more popular direct methods (refs. 1-7). MRAC methods adaptively tune the controller gains, forcing the actual system to follow some ideal reference model. Because this reference model can be of lower order than a typical model of the actual system, this method is very attractive for applications to LSS, where structural models can be of very high order and require truncation for use with any controller. Figure 1 shows a block diagram of a generalized MRAC system (ref. 6).

PROBLEM FORMULATION

The LSS, or controlled plant can be represented in standard state space form:

$$\dot{X}_p(t) = A_p X_p(t) + B_p U_p(t) \tag{1a}$$

$$Y_p(t) = C_p X_p(t) \tag{1b}$$

where $X_p \epsilon R^{Np}$, $U_p \epsilon R^M$, $Y_p \epsilon R^M$ and A_p, B_p, C_p are of appropriate dimensions. It is assumed that (A_p, B_p) is controllable, (A_p, C_p) is observable, and that the number of inputs (M) is equal to the number of outputs.

A stable reference model which specifies the desired performance of the plant is also described by a state space representation,

$$\dot{X}_m(t) = A_m X_m(t) + B_m U_m(t) \tag{2a}$$

$$Y_m = C_m X_m(t) \tag{2b}$$

where $X_m \in R^{Nm}$, $U_m \in R^M$, $Y_m \in R^M$ and A_m, B_m, C_m are of appropriate dimensions. For practical application to LSS the following condition must be true

$$N_p >> N_m \tag{3}$$

To aid in measuring how close the actual plant is to the reference model, the output error between the plant and the reference model is defined as

$$e_y(t) = Y_m(t) - Y_p(t) \tag{4}$$

Since the output error tells us how close the actual plant is to the desired performance of the reference model, the objective of any adaptive update scheme is to design a control input which forces the output error to zero asymptotically.

ADAPTIVE LAW

The adaptive mechanism used in this paper is based on the work of Sobel, Kaufman and Mabius (ref. 1) and has no provisions for the destabilizing effects of noise. However, it has found important application to LSS. The control input is written as,

$$U_p(t) = K(t)\,r(t) \tag{5}$$

where

$$r^T = \left[e_y^T, X_m^T, U_m^T\right] \tag{6a}$$

$$K(t) = \left[K_e(t), K_x(t), K_u(t)\right] \tag{6b}$$

The adaptive gain K(t) is calculated as the sum of a proportional component $K_{pr}(t)$ and an integral component $K_I(t)$ so that

$$K(t) = K_{pr}(t) + K_I(t) \tag{7}$$

The adaptive laws for $K_{pr}(t)$ and $K_I(t)$ are given as

$$K_{pr}(t) = e_y r^T T^* \tag{8}$$

$$\dot{K}_I(t) = e_y r^T T \tag{9}$$

where T^* and T are time invariant weighting matrices of appropriate dimension chosen by the designer. Sufficient conditions for global stability are presented in (ref 1-3, 11-12) and will only be summarized here.

1. $$T \;\&\; T^* > 0$$
2. there exist $P = P^T > 0$ and $Q = Q^T > 0$ such that

$$PB_p = C_p^T$$

$$PA_p + A_p^T P = -Q$$

Condition 1 is met simply by choosing appropriate matrices (i.e., the identity matrix). Condition 2 is equivalent to the assumption that the open-loop plant transfer function matrix

$$Z(s) = C_p(sI - A_p)^{-1}B_p \tag{10}$$

is strictly positive real. This condition is met for any LSS having small but non-zero inherent damping and colocated sensors and actuators.

CONTROL EFFORT

In order to assess the added implementation costs of MRAC in systems where reasonable amounts of error would occur, we have adopted the following procedure. The first step is to choose a linear system to represent the actual physical system. Next, we create a reference model which specifies the desired performance and has some measurable amount of error. Previous examples, see (ref. 2), have chosen the reference model to be a reduced model of the actual plant with the same frequencies and mode shapes plus extra damping. While this would be the ideal situation, it is not probable that we would have an exact theoretical model. For this reason we have intentionally introduced errors between our reference models and the actual plant model. To aid in quantifying the increased effort due to the errors, we calculate the following performance indices:

the maximum control force required by each actuator,

$$U_i^{max} = \mathrm{Max}(\ |\ U_i(t)\ |\ ) \quad 0 \le t \le t_{final},\ \ i = 1,\ldots,M \tag{11}$$

the quadratic control effort,

$$U_{total} = \int U^T U dt \tag{12}$$

the integral of the potential energy of the system,

$$PE = \frac{1}{2}\int X^T K X dt \tag{13}$$

and the integral of the kinetic energy

$$KE = \frac{1}{2}\int \dot{X}^T M \dot{X} dt \tag{14}$$

where the first two performance indices measure the control effort and the second two provide information about system response characteristics. These performance indices allow us to see how increments of error affect the cost and performance of the system.

SIMPLY SUPPORTED BEAM EXAMPLE

The first example is a simply supported beam with a variable concentrated mass at the mid-span and a velocity sensor and force actuator colocated at one-sixth span (see figure 2). This simple structure is similar to a structure used by Bar-Kana, Kaufman & Balas (ref. 2) for demonstrating the MRAC method. The only difference between the present structure and the structure of reference 2 is the variable concentrated mass. The variable concentrated mass at the mid-span was used to create error in the system due to unknown mass characteristics. The concentrated mass was varied between 0-20% of the mass of the beam, with zero mass corresponding to an exact reference model. It should be noted that the reference model was held constant while the plant model was varied to match changes in the concentrated mass.

The beam was modeled with 12 beam finite elements with a displacement and rotational Degree of Freedom (DOF) at each nodal point. The coupled equations of motion are written in standard form as

$$M\ddot{q} + C\dot{q} + Kq = F \tag{15}$$

where M and K are the mass and stiffness matrices respectively, and C is the damping matrix calculated from assumed inherent damping ratios ζ_i. Using modal analysis the equations are transformed from a set of coupled equations in physical coordinates to a set of coupled equations in physical coordinates to a set of uncoupled equations in modal coordinates

$$\ddot{X} + 2\zeta\omega\dot{X} + \Lambda X = B^{o}F \tag{16}$$

where

$$\Lambda = \mathrm{diag}[\omega_1^2, \omega_2^2, \ldots \omega_{12}^2]$$

the ω_i's are the undamped natural frequencies

$$\zeta\omega_n = \mathrm{diag}[\zeta_1\omega_1, \zeta_2\omega_2, \ldots, \zeta_{12}\omega_{12}]$$

$$B^{o} = [\phi_{5,1}, \phi_{5,2}, \ldots, \phi_{5,12}]^T$$

and the $\phi_{5,i}$'s are the fifth element of each eigenvector (the sensor and actuator are at the 5^{th} DOF) normalized so

$$\Phi^T M \Phi = I$$

Equation 16 is rewritten in state space form as

$$\begin{bmatrix}\ddot{X}_p \\ \dot{X}_p\end{bmatrix} = \begin{bmatrix}-2\zeta_p\omega_{np} & -\Lambda_p \\ I & 0\end{bmatrix}\begin{bmatrix}\dot{X}_p \\ X_p\end{bmatrix} + \begin{bmatrix}B_p^{o} \\ 0\end{bmatrix}U_p \tag{17a}$$

$$Y_p = \begin{bmatrix}B_p^{oT} & 0\end{bmatrix}\begin{bmatrix}\dot{X}_p \\ X_p\end{bmatrix} \tag{17b}$$

where the subscript p denotes the equations apply to the plant. The reference model takes the same form,

$$\begin{bmatrix}\ddot{X}_m \\ \dot{X}_m\end{bmatrix} = \begin{bmatrix}-2\zeta_m\omega_{nm} & -\Lambda_m \\ I & 0\end{bmatrix}\begin{bmatrix}\dot{X}_m \\ X_m\end{bmatrix} + \begin{bmatrix}B_m^{o} \\ 0\end{bmatrix}U_m \tag{18a}$$

$$Y_m = \begin{bmatrix}B_m^{oT} & 0\end{bmatrix}\begin{bmatrix}\dot{X}_m \\ X_m\end{bmatrix} \tag{18b}$$

where the subscript m applies to the reference model.

For the purpose of numerical simulations we must reduce the size of the actual plant. In this example (as in ref. 2) we consider only the first three modes of the actual plant and choose a reference model that includes only 2 modes. Damping ratios in the plant are assumed to be 0.01 while the desired damping ratios of the reference model are set at 0.05. All other parameters (length, EI, etc.) are set to 1.0 for convenience in calculations. In the present study we consider only initial condition responses. The first three modal states were initially set to 1.0, while all others were set to zero. From figures 3-4 it can be seen that the controller does an excellent job of forcing the actual plant to follow the reference model. However, from Table 1 it can be seen that the addition of the concentrated mass, i.e. errors between the actual plant and the reference model, can produce very large increases in the maximum control force and control effort needed for the controller to function. For example, a concentrated mass weighing 20% of the beam weight causes a factor of six increase in the quadratic control effort. This large increase in control effort demonstrates a need to find a method for choosing a good reference model.

SLEWING GRID EXAMPLE

The Virginia Tech slewing grid laboratory structure shown in figure 5 is a more complex example. The slewing grid was designed to have characteristics of LSS, namely closely spaced modes, low vibration frequencies, and low inherent damping. Three pairs of velocity sensors and force actuators are colocated at joints 3,4 &5. The slewing grid was designed to include a zero frequency rigid body rotation mode about the shaft, but this has never been realized because of bearing friction and slight misalignments of the rotational shaft. Although the geometry of the structure is symmetric about a horizontal line through joint 3, the vibration mode shapes are not similarly symmetric because the structure's weight causes asymmetric member gravity loading and therefore asymmetric stiffness distribution. It was considered desirable in the design phase to have at least one beam member in substantial compression relative to its buckling load, both to reduce the overall structural stiffness and to permit the possibility of nonlinear response. The lower horizontal member carries the largest compressive load, being compressed to about 70% of its Euler (pin-ended) buckling load. Great effort has been taken to accurately predict the loads in each member of the structure. However, each joint is held in place with a nut and bolt assembly and the process of tightening these bolts induces forces which we have been unable to determine accurately. Therefore our current Finite Element Model (FEM) only takes gravity forces into account. The rotational shaft was modeled by 8 beam finite elements with a displacement and rotation DOF at each node. Each of the 5 members of the structure is modeled with 4 finite elements which include a transverse displacement, an in-plane rotation, and an out of plane rotation at each node. The complete FEM has 72 DOF and the coupled equations of motions can be written

$$M\ddot{X} + C\dot{X} + (K + G)X = F \tag{19}$$

where G is the geometric stiffness matrix. To make the problem more manageable we created a reduced eleventh order model using the Guyan Reduction (ref. 15). The linear equations for the slewing grid can be written (in physical coordinates)

$$\begin{bmatrix} \ddot{X}_p \\ \dot{X}_p \end{bmatrix} = \begin{bmatrix} -M_p^{-1}C_p & -M_p^{-1}\overline{K_p} \\ I & 0 \end{bmatrix} \begin{bmatrix} \dot{X}_p \\ X_p \end{bmatrix} + \begin{bmatrix} B_p \\ 0 \end{bmatrix} U_p \tag{20a}$$

$$Y_p = \begin{bmatrix} B_p^T & 0 \end{bmatrix} \begin{bmatrix} \dot{X}_p \\ X_p \end{bmatrix} \tag{20b}$$

where

$$\overline{K_p} = K_p + G_p \tag{21}$$

M_p, C_p, K_p, and G_p are the reduced mass, damping, stiffness and geometric stiffness matrices, and B_p is (22 X 3) matrix with only 3 non-zero elements for mapping the control inputs to the proper DOF at joints 3,4,5.

The accuracy of the frequencies and modes predicted by the FEM is not good. During the past two years, great pains have been taken to find a FEM which would accurately model the structure. However all the non-linearities in the structure, such as friction in the bearing, large gravity loading in the lower horizontal member, and the loads induced by tightening the bolts at each joint of the structure, have resulted in a modeling nightmare. Table 2 compares frequencies predicted by our best FEM to the experimental vibration frequencies, and figures 6-9 compare several experimental and theoretical mode shapes. The difficulty in accurately modeling this structure was the driving force behind the decision to apply adaptive control to the slewing grid. The challenges of modeling the slewing grid may be similar to those we will face when we begin to model LSS.

In order to study the performance of MRAC for this case we first had to choose a model for simulating the actual plant. Our efforts to model the slewing grid as accurately as possible resulted in several FEM with varying degrees of accuracy. The most accurate model used experimental frequencies and mode shapes in a correction method proposed by Baruch (ref.16) to force the theoretical model to have exact experimental frequencies. The least accurate model was the standard FEM with no corrections. With this in mind we chose the most accurate FEM to simulate the plant and a linear combination of the most accurate and least accurate model as the reference model. The reference model is described by the following equation.

$$Ref.Model = \alpha(standard\ FEM) + (1-\alpha)(corrected\ model) \tag{22}$$

Thus we can vary the amount of error between the reference model and the actual model and monitor the control effort and system response as the error increases (α = 0---Perfect Modeling , α = 1--- Max. Error). Damping ratios for the simulated plant were obtained experimentally, while the damping ratios for the reference model specify the desired performance (see table 3).

In addition to varying the parameter α, we also varied the initial conditions of the structure. In the first simulation the structure was deformed into the second mode shape (see figure 6) and released. Table 4 shows that introducing errors into the reference model had a significant effect on the maximum force at joint 3 and the quadratic control effort. The maximum force required at joint 3 is 10 times larger at α = 1.0 than at α = 0.0, and the quadratic control effort is increased by a factor of 27 over the same interval. In the second simulation the structure was deformed into the theoretical fourth mode shape (see figure 8) and released. Table 5 shows that introducing errors in this case also causes dramatic increases in control costs. For example, at the point of maximum error (α = 1), the total control effort needed increased by almost 2500%, the maximum control force required by actuator 3 increased over 600%, and the amount of potential and kinetic energy in the system increased over 550%.

CONCLUDING REMARKS

The performance of Model Reference Adaptive Control (MRAC) was studied in numerical simulations with the objective of understanding the effects of differences between the plant and the reference model. MRAC was applied to two structural systems with controlled error between the reference model and the actual plant. Performance indices relating to control effort and response characteristics were monitored in order to determine what effects small errors have on the control effort and performance of the two systems. It was shown that reasonable amounts of error in the reference model can cause dramatic increases in both the control effort and and response magnitude (as measured by energy integrals) of the plant.

ACKNOWLEDGEMENT

This work was supported in part by NASA grant NAG-1-603

REFERENCES

1. Sobel, K., Kaufman, H., and Mabius, L., "Implicit Adaptive Control Systems for a Class of Multi-Input Multi-Output Systems," IEEE Transactions on Aerospace and Electronics Systems, Sept. 1982, pp. 576-590.

2. Bar-Kana, Kaufman, H., and Balas, M., "Model Reference Adaptive Control of Large Structural Systems," Journal of Guidance and Control 1983, Vol. 6, No. 2, pp.112-118.

3. Mufti, H., "Model Reference Adaptive Control for Large Structural Systems," Journal of Guidance and Control 1987, vol 10, No. 5, pp.507-509.

4. Ih, C-H.C., D. S. Bayard, and S. J. Wang, "Space Station Adaptive Payload Articulation Control," In Fourth IFAC Symposium on Control of Distributed Parameter Systems, Los Angles, CA, July 1986.

5. Bayard, D. S., C-H.C. Ih, and S. J. Wang, "Adaptive Control for Flexible Structures with Measurement Noise,: Proc. American Control Conference, Minneapolis, MN, pp.368-379, June 10-12 1987.

6. R. D. Nussbaum, "Some Remarks on a Conjecture in Parameter Adaptive Control," Systems and Control Letters, Vol. 3, No. 5 pp, 243-246, 1983.

7. J. C. Willems and C. I. Byrnes, "Global Adaptive Stabilization in the Absence of Information on the sign of the High Frequency Gain." Proc. INRIA Conf. on Analysis and Optimization of Systems, Springer-Verlag, 1984, pp.49-57.

8. C. I. Byrnes, and J. C. Willems, "Adaptive Stabilization of Multivariable Linear Systems,": IEEE Proc. 23 Conf. Decision and Control, 1984, pp. 1574-1577.

9. R. L. Kosut, "Adaptive Control of Large Space Structures," Proc. of the 5th AFOSR Forum on Space Structures, pp. 51-55, Aug. 20-21, 1987.

10. R. H. Middleton, G. C. Goodwin, D. J. Hill, and D. Q. Mayne, "Design Issues in Adaptive Control," IEEE Transactions on Automatic Control, Vol. 33, No. 1, pp.50-57, Jan, 1988.

11. N. Sundararajan, J. P. Williams, and R. C. Montgomery, "Adaptive Modal Control of Structural Dynamic Systems Using Recursive Lattice Filters," Journal of Guidance and Control, Vol. 8, No. 2, pp. 223-229, March-April, 1985.

12. C-H.C. Ih, D. S. Bayard, S. J. Wang, and D. B. Elder, "Adaptive Control Experiment With a Large Flexible Structure,:AIAA Guidance, Navigation and Control Conference, Paper AIAA-88-4153 -CP, Minneapolis, MN, Aug 15-17, 1988.

13. C-H.C. Ih, D. S. Bayard, A. Ahmed, and S. J. Wang, "Experiments in Multivariable Adaptive Control of a Large Flexible Structure," AIAA Guidance, Navigation and Control Conference, Boston, MA, Aug. 1989.

14. W-W. Chiang, and R. H. Cannon, Jr, "The Experimental Results of a Self Tuning Adaptive Controller Using Online Frequency Identification," The Journal of the Astronautical Sciences, Vol. 33, No. 1, Jan-Mar, 1985, pp. 71-83.

15. R. J. Guyan, "Reduction of Stiffness and Mass Matrices", AIAA Journal, Vol. 3, No 2, Feb. 1965.

16. M. Baruch, "Optimal Correction of Mass and Stiffness Matrices Using Measured Modes", AIAA Journal, Mol. 20, 1982, pp. 1623-1626.

TABLE 1

SUMMARY OF PERFORMANCE MEASURES FOR VARYING AMOUNTS OF MASS ERROR IN THE SIMPLY SUPPORTED BEAM EXAMPLE

% ERROR	MAXIMUM FORCE	TOTAL QUADRATIC CONTROL EFFORT
0.0	380	11,422
10.0	540	27,486
20.0	920	72,263

TABLE 2

SUMMARY OF THEORETICAL VS EXPERIMENTAL FREQUENCIES FOR THE SLEWING GRID STRUCTURE

MODE #	FREQUENCIES (Hz)		% ERROR
	THEORETICAL	EXPERIMENTAL	
1	0.36	0.42	16.67
2	1.37	1.45	5.84
3	3.00	2.88	4.00
4	4.47	5.39	20.58
5	6.02	6.41	6.48
6	6.69	6.88	2.84
7	9.79	9.05	7.56
8	11.52	10.18	11.63
9	13.11	13.56	3.43
10	15.35	14.90	2.93
11	21.16	15.37	27.36

TABLE 3

DAMPING RATIOS FOR THE MODELS OF THE SLEWING GRID

MODE #	EXPERIMENTAL FREQUENCY (HZ)	EXPERIMENTAL DAMPING RATIOS	DAMPING RATIOS FOR THE REF. MODEL
1	0.42	0.110	0.15
2	1.45	0.015	0.05
3	2.88	0.011	0.05
4	5.39	0.008	0.05
5	6.41	0.003	0.05
6	6.88	0.011	0.05
7	9.05	0.003	0.05
8	10.18	0.003	0.05
9	13.56	0.002	0.01
10	14.90	0.002	0.01
11	15.37	0.002	0.01

TABLE 4

SUMMARY OF PERFORMANCE MEASURES FOR VARYING AMOUNTS OF ERROR IN THE SLEWING GRID
INITIAL CONDITIONS = MODE SHAPE 2

ALPHA	MAXIMUM FORCE (LBS)			QUADRATIC CONTROL EFFORT LBS^2-SEC	KINETIC ENERGY INTEGRAL LB-IN-SEC	POTENTIAL ENERGY INTEGRAL LB-IN-SEC
	JT. 3	JT. 4	JT. 5			
0.00	0.0182	0.022	0.021	0.00044	0.116	0.117
0.25	0.0596	0.028	0.025	0.00107	0.114	0.119
0.50	0.1090	0.038	0.035	0.00299	0.112	0.120
0.75	0.1520	0.048	0.045	0.00742	0.111	0.122
1.00	0.1825	0.057	0.058	0.01250	0.110	0.125

TABLE 5

SUMMARY OF PERFORMANCE MEASURES FOR VARYING AMOUNTS OF ERROR IN THE SLEWING GRID
INITIAL CONDITIONS = MODE SHAPE 4

ALPHA	MAXIMUM FORCE (LBS)			QUADRATIC CONTROL EFFORT LBS^2-SEC	KINETIC ENERGY INTEGRAL LB-IN-SEC	POTENTIAL ENERGY INTEGRAL LB-IN-SEC
	JT. 3	JT. 4	JT. 5			
0.00	0.44	0.68	0.58	0.35	0.60	0.60
0.25	0.58	0.78	0.64	0.52	0.70	0.72
0.50	1.19	0.93	0.72	1.47	1.09	1.13
0.75	2.42	1.04	0.89	5.20	2.49	2.55
1.00	3.12	1.04	0.90	9.05	3.94	3.93

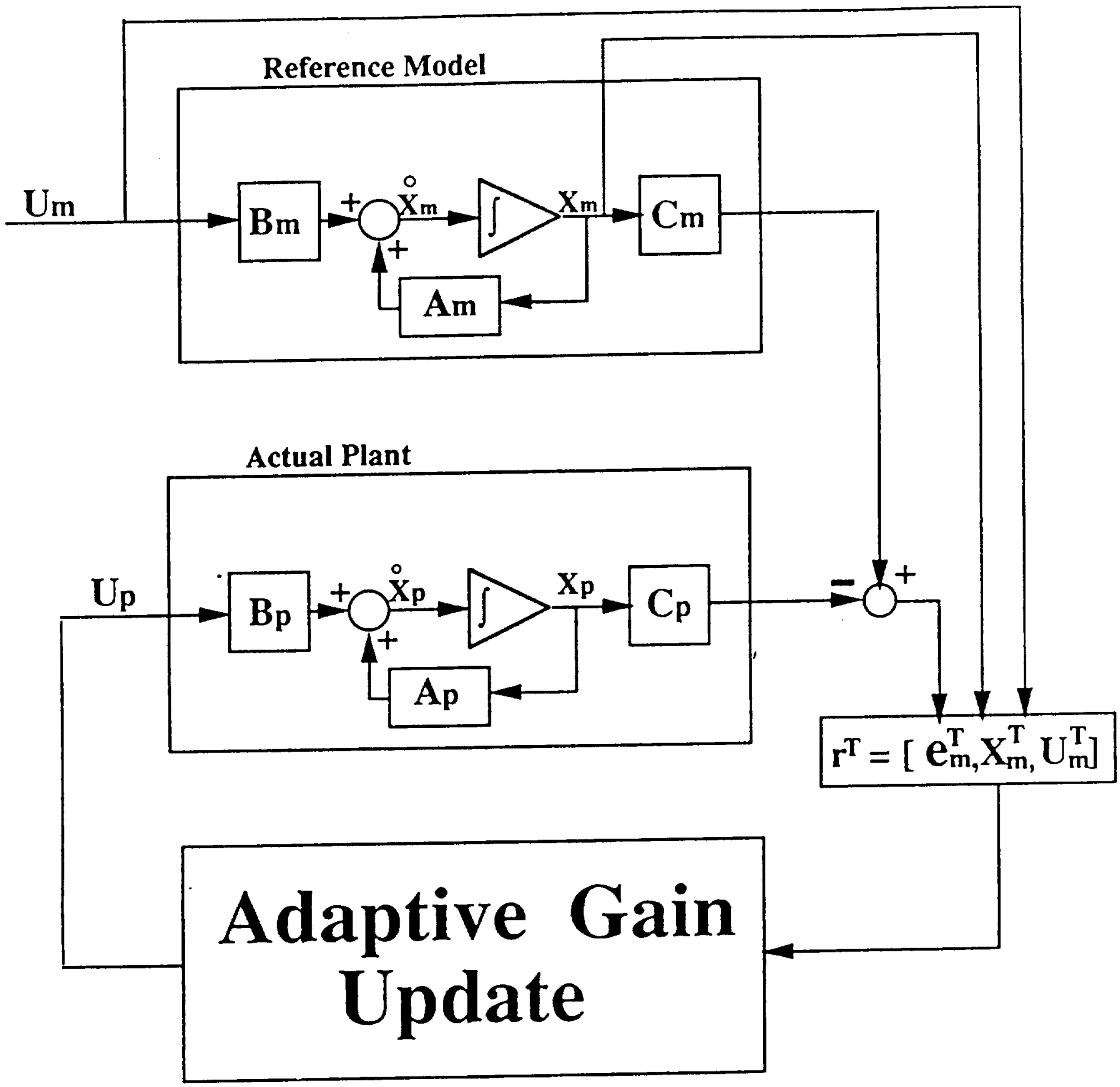

Figure 1

MODEL REFERENCE ADAPTIVE CONTROL BLOCK DIAGRAM

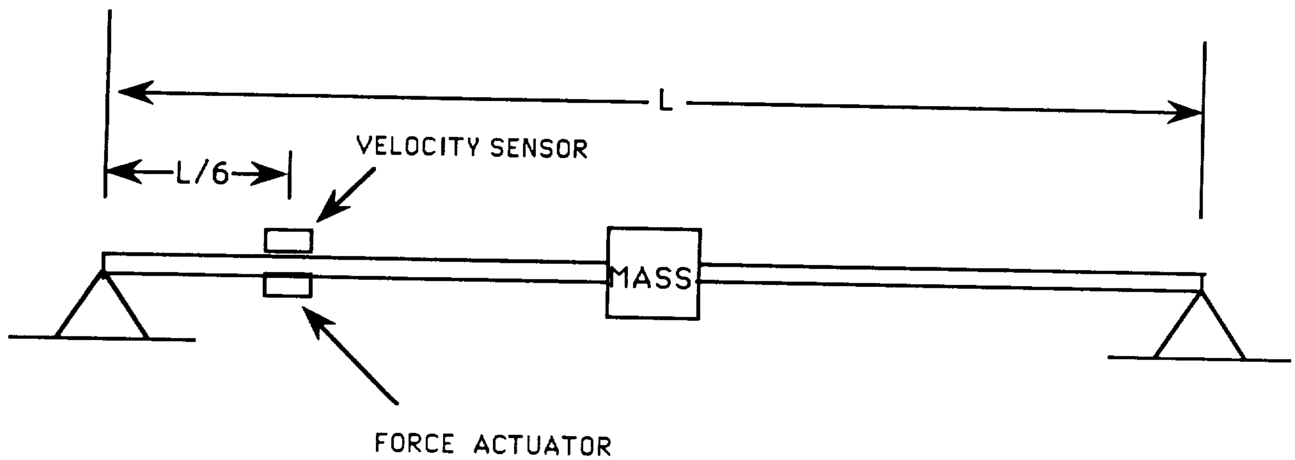

Figure 2

SIMPLY SUPPORTED BEAM WITH
VARIABLE CONCENTRATED MASS

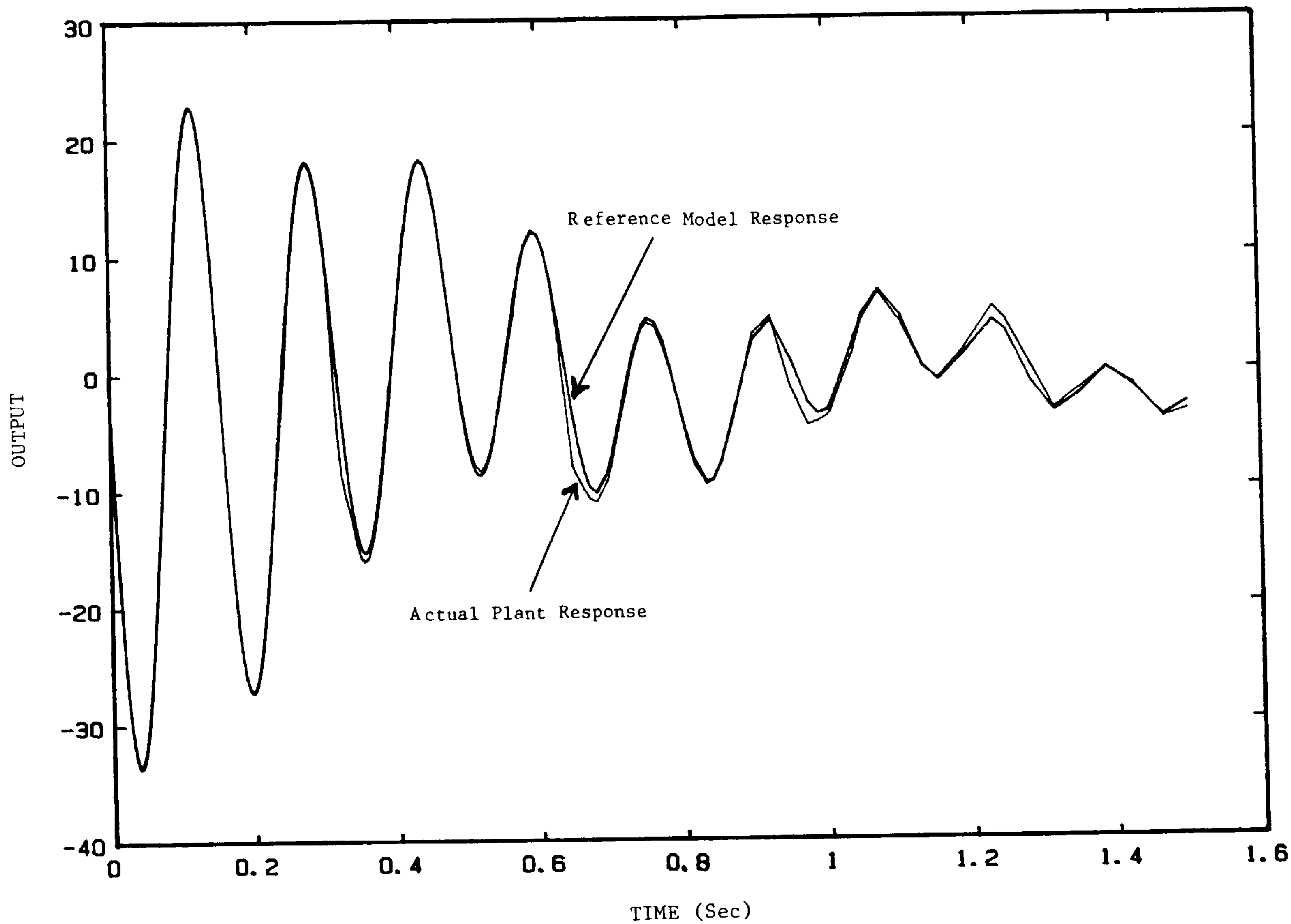

Figure 3
VELOCITY RESPONSE AT THE SENSOR LOCATION FOR THE BEAM STRUCTURE WITH A 10% CONCENTRATED MASS

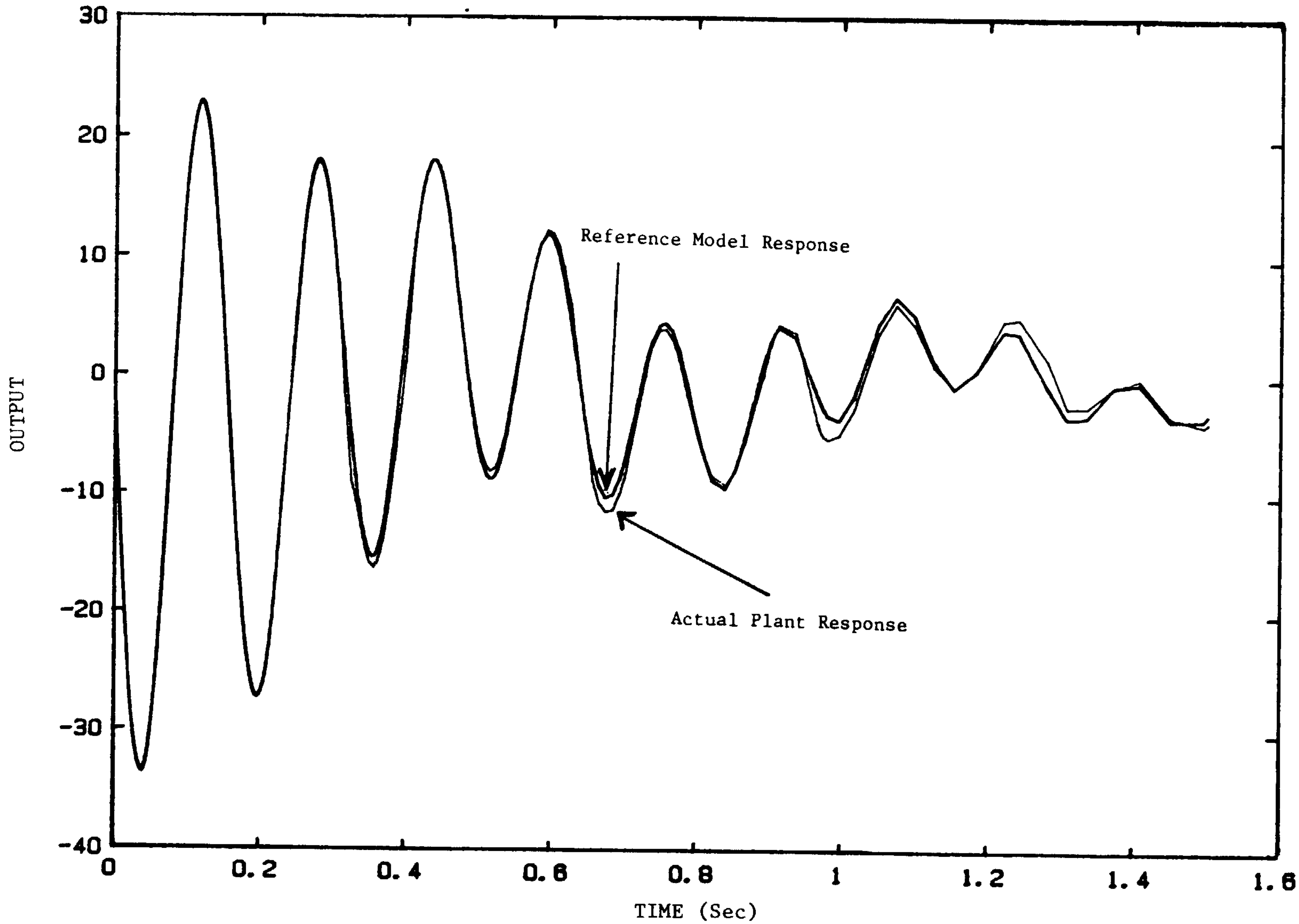

Figure 4
VELOCITY RESPONSE AT THE SENSOR LOCATION FOR THE BEAM STRUCTURE WITH A 20% CONCENTRATED MASS

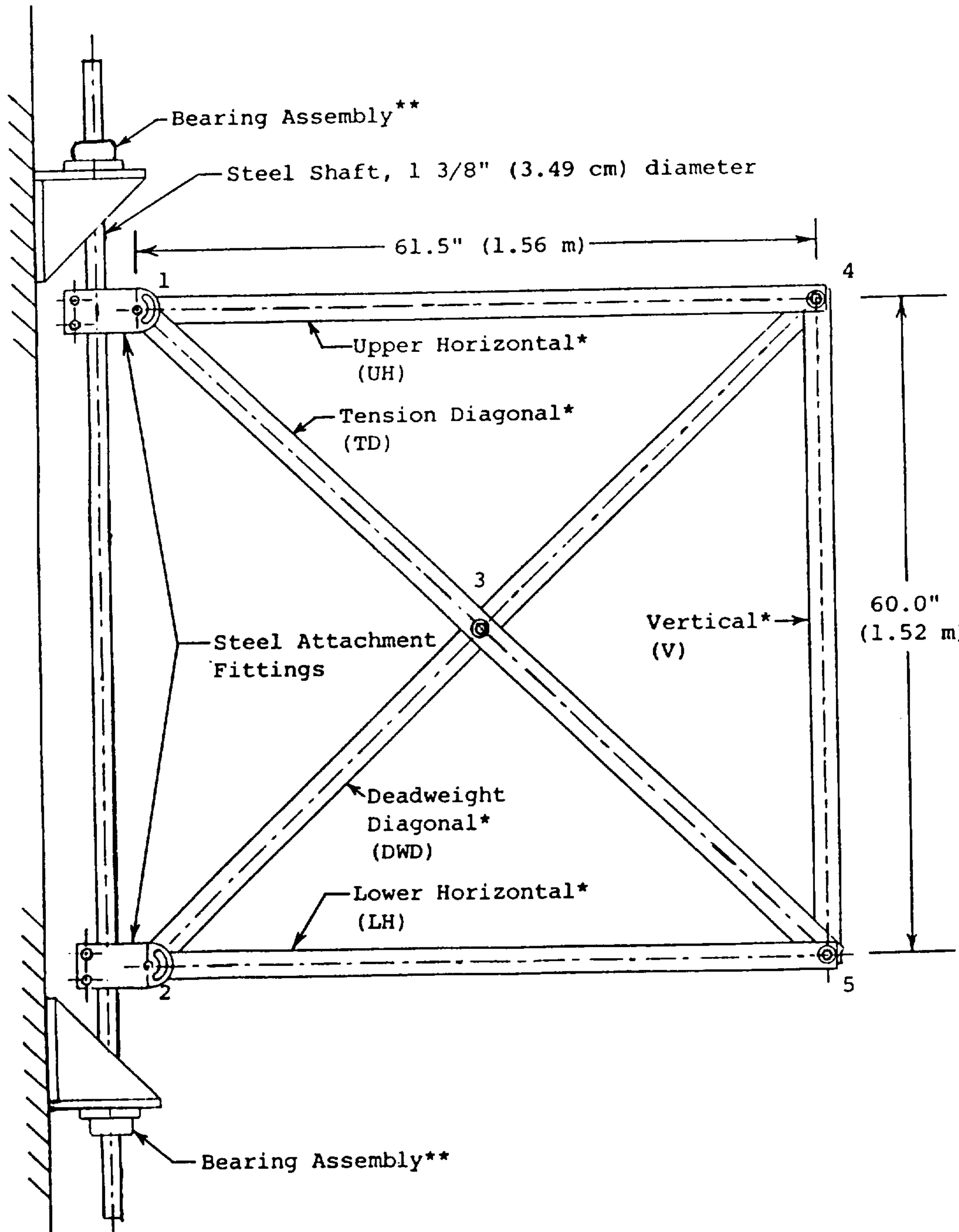

*Aluminum Beam Members
Alloy 6061-T6
Nominal cross-section:
2" x 1/8"
(5.08 cm x 0.32 cm)

**Ball Bearings
Make: SKF
Bearing No. 478207-106
Pillow Block Flange Unit
No. FYP-106
(Bearing seals and all grease were removed to reduce friction.)

Figure 5
SLEWING GRID STRUCTURE

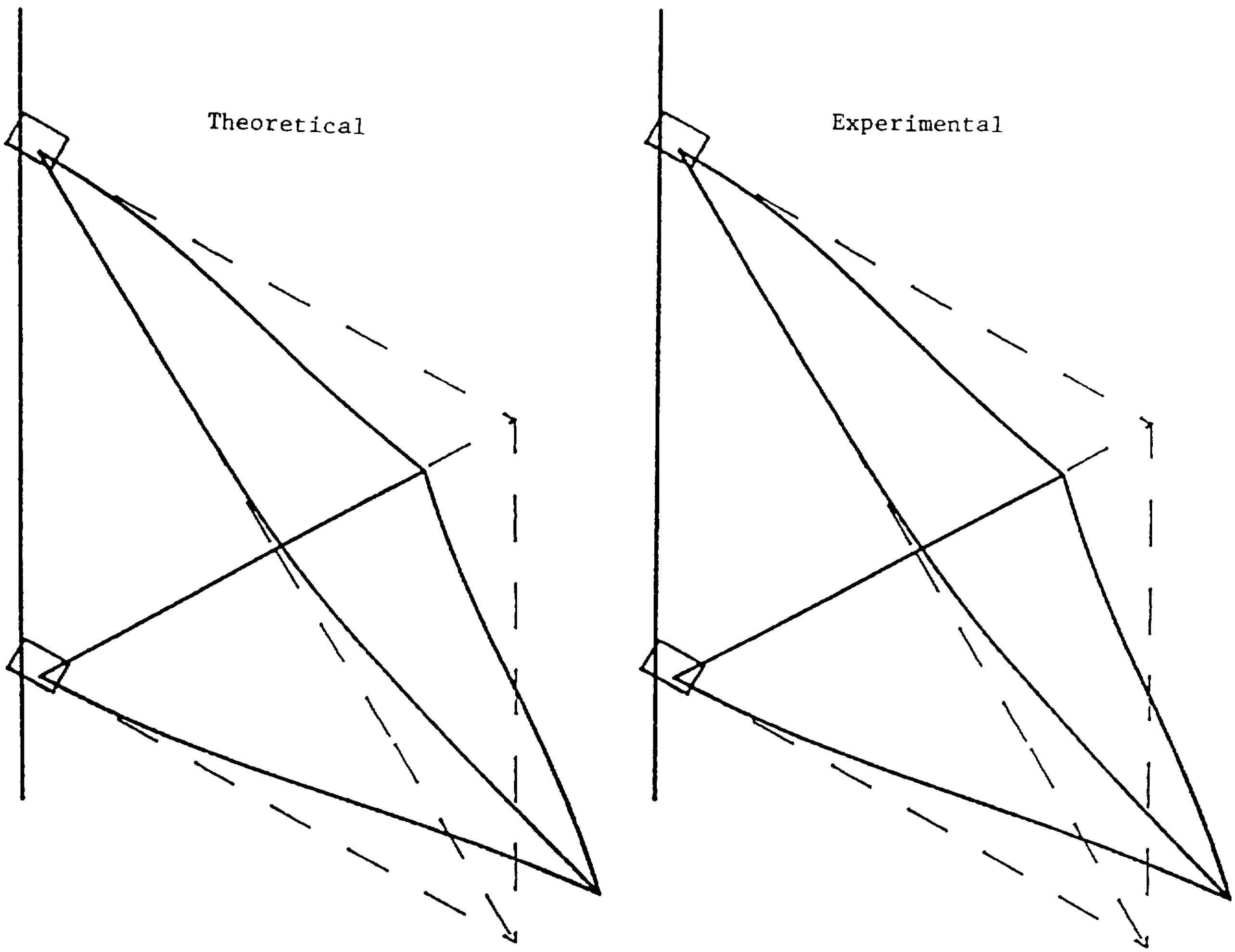

Figure 6

SECOND MODE SHAPE FOR SLEWING GRID STRUCTURE

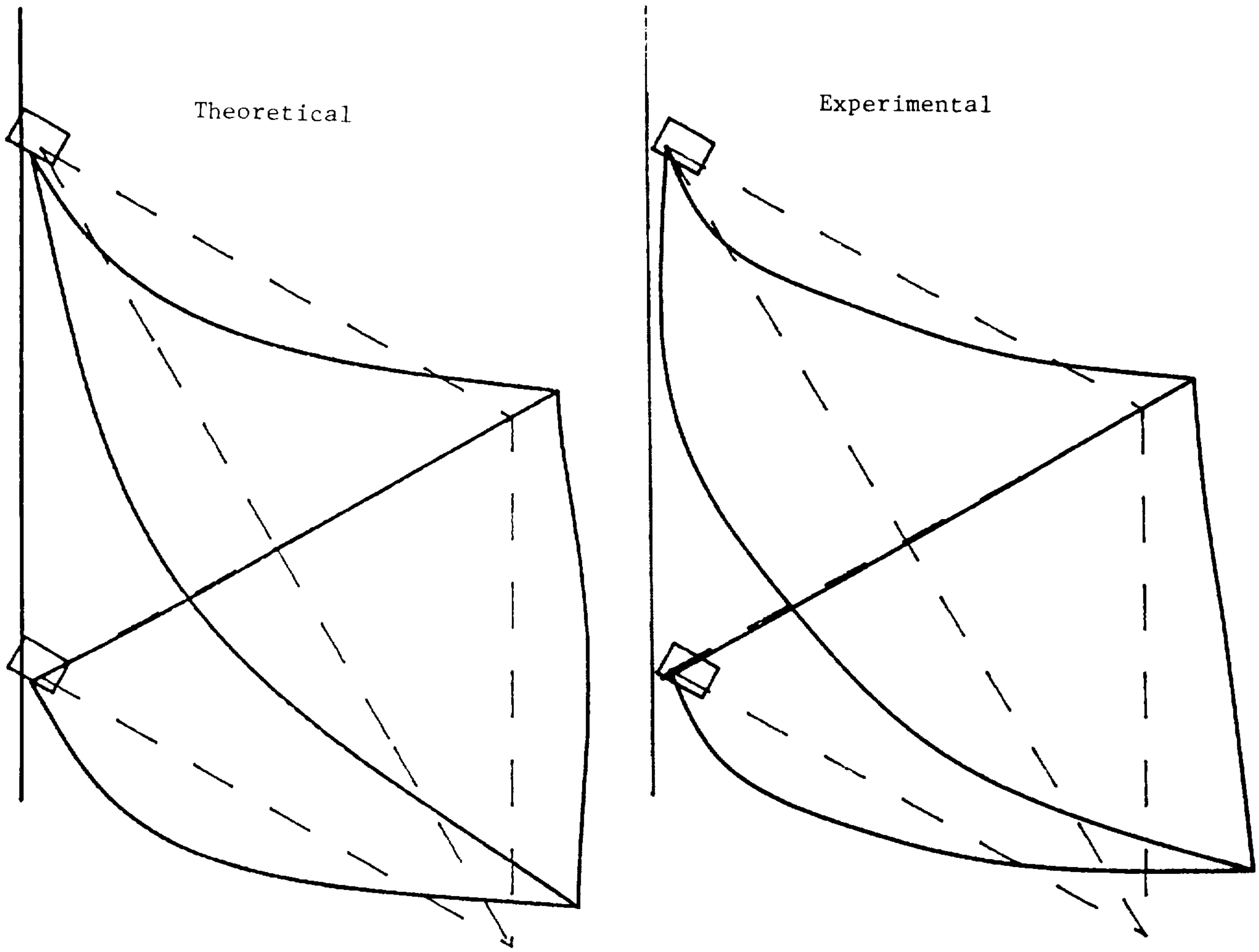

Figure 7

THIRD MODE SHAPE FOR SLEWING GRID STRUCTURE

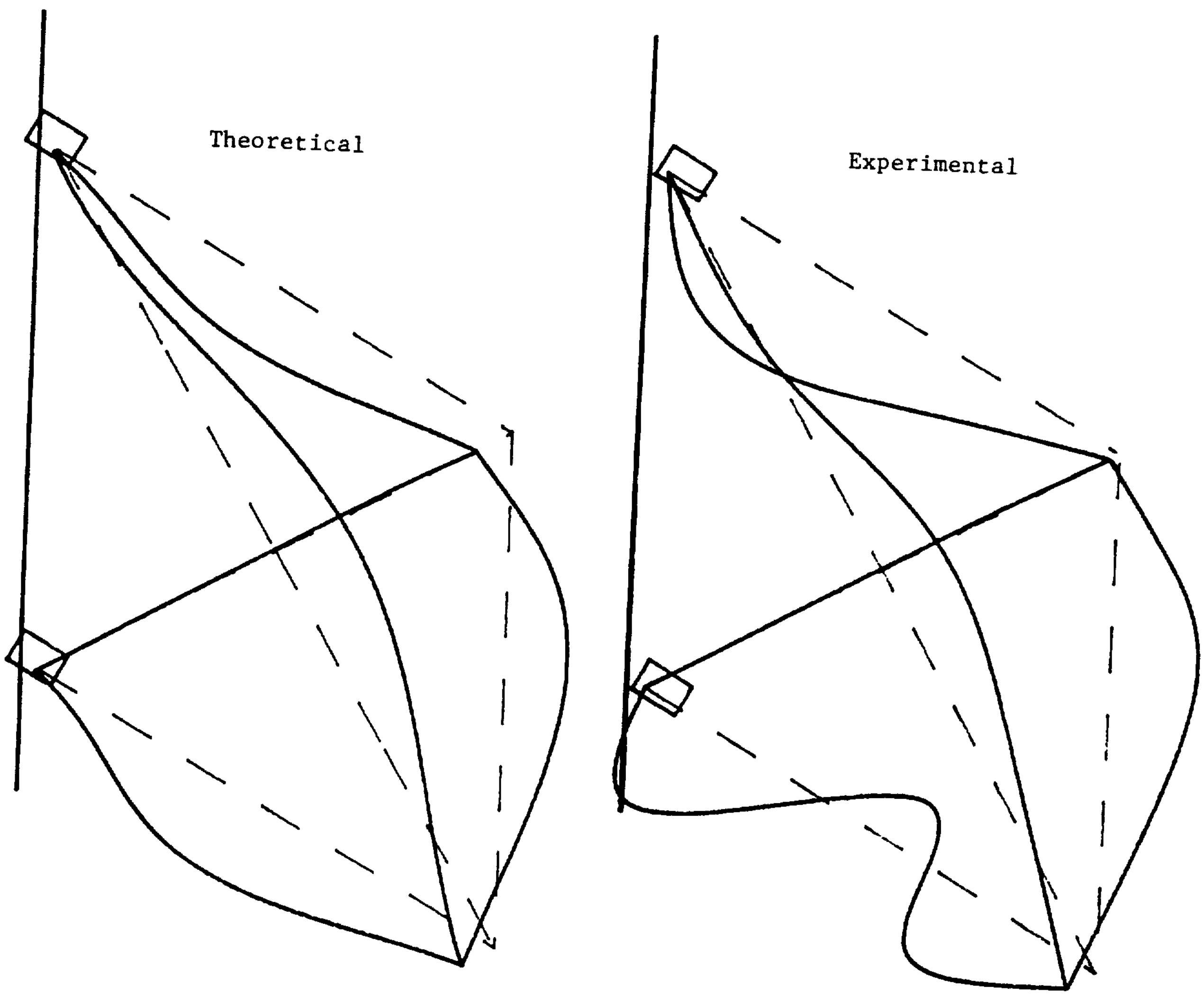

Figure 8

FOURTH MODE SHAPE FOR SLEWING GRID STRUCTURE

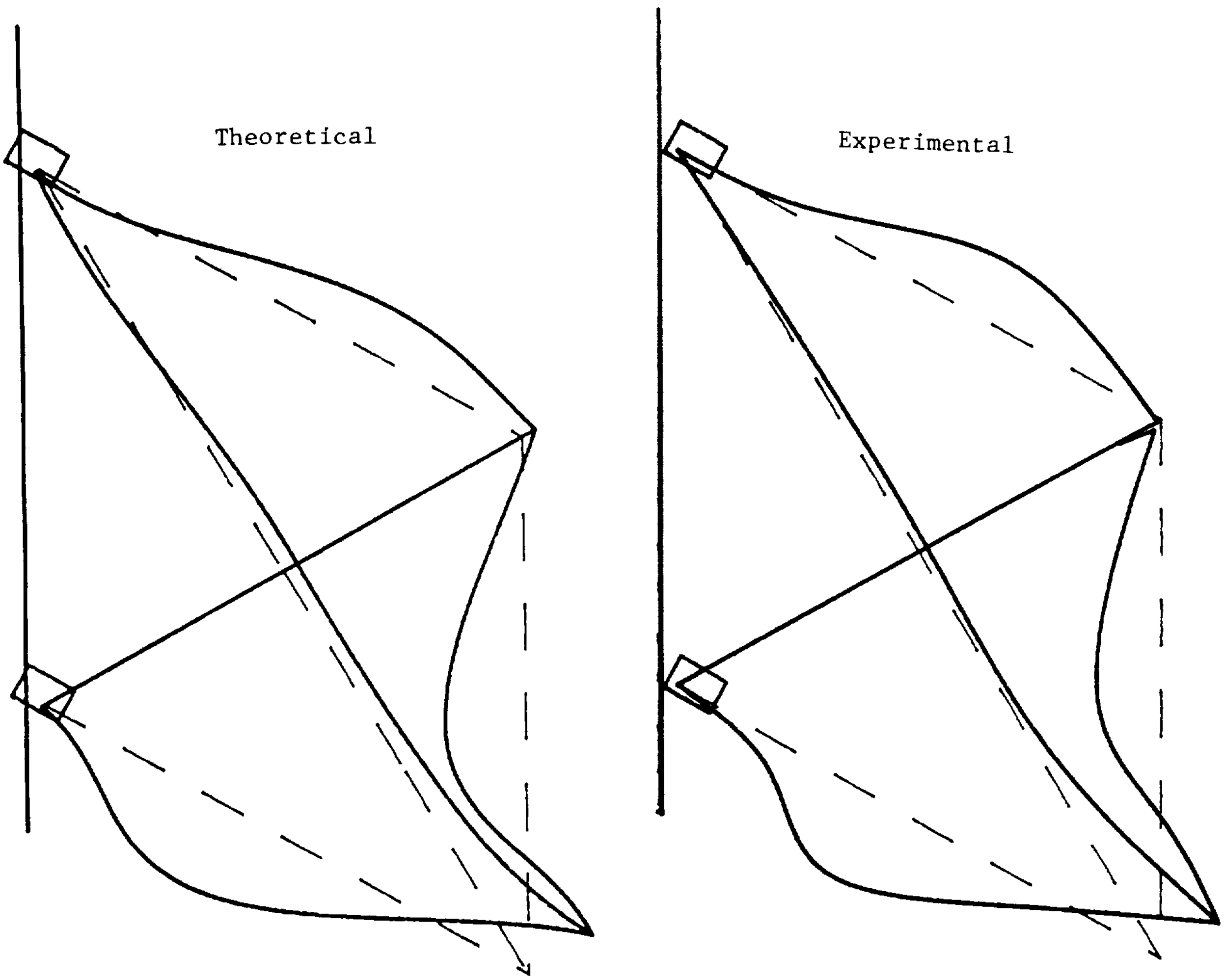

Figure 9

FIFTH MODE SHAPE FOR SLEWING GRID STRUCTURE